

# SENSOR OPTIMAL IMAGE INTERPOLATION

Jeffery R. Price

IRIS Lab, Dept. of ECE  
University of Tennessee  
Knoxville, TN  
jrp@utk.edu

Monson H. Hayes III

CSIP, School of ECE  
Georgia Institute of Technology  
Atlanta, GA  
monson.hayes@ece.gatech.edu

## ABSTRACT

Previously, we derived sensor optimal prefilters for image interpolation. The prefilters were applied prior to integer interpolation with a standard (e.g., linear or cubic) kernel. Here we expand upon that notion and construct complete, sensor optimal interpolation kernels for rational interpolation factors. After restating the interpolation problem in a reconstruction-like fashion, we employ a simple model of the image capture system to derive the MMSE interpolator. Results indicate significant subjective improvements over cubic interpolation, for little extra computation.

## 1. INTRODUCTION

Image interpolation is an important task in many applications. Some examples include professional and consumer imaging software as well as texture mapping for 3D scene reconstruction. If information about the system used to capture a given image is known, it seems reasonable to expect that such information could be used to improve the interpolation of that image. As noted in [1], other researchers [2, 3] have considered this problem before, although in a different fashion than we do. A similar approach to what we present here can be found in [4]. Our technique differs from [4] in that we employ a *nonseparable* image covariance model and additionally construct the interpolation kernels in the spatial domain – the Wiener restoration filters in [4] are found in the Fourier domain, windowed, then sampled to provide the spatial domain kernels.

To use knowledge of the capture system, we first pose the image interpolation problem in a reconstruction-like manner as follows: *The given*

This work was supported by a Kodak Fellowship and by DOE's University Research Program in Robotics (URPR) under grant DOE-DE-FG02-86NE37968.

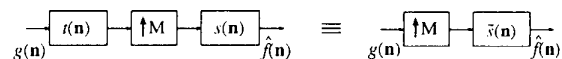


Figure 1: Equivalent forms of optimal prefiltering followed by integer interpolation.

*image is the observation of a scene captured by a low resolution sensor. An interpolated image is sought that is an observation of the same scene, captured by a higher resolution sensor. Such an interpretation has been previously mentioned in [2, 3, 5, 6].*

## 2. PROBLEM FORMULATION

In the optimal prefiltering approach from [1], we applied a prefilter, upsampled (by an integer factor), and then interpolated. When the interpolation is implemented by a linear, shift invariant filter (e.g., cubic or linear interpolation), the entire process is equivalent to upsampling and filtering with a modified interpolation kernel, as shown in Fig. 1. The modified interpolation kernel,  $\bar{s}(\mathbf{n})$ , is given by

$$\bar{s}(\mathbf{n}) = (t_M * s)(\mathbf{n}) \quad (1)$$

where  $t_M(\mathbf{n})$  is the prefilter,  $t(\mathbf{n})$ , upsampled by a factor of  $M$ :

$$t_M(\mathbf{n}) = \begin{cases} t(\mathbf{n}/M) & ; \mathbf{n} = M\mathbf{k}, \mathbf{k} \in \mathbb{Z} \times \mathbb{Z}, \\ 0 & ; \text{otherwise.} \end{cases} \quad (2)$$

With this in mind, a more complete approach is to find an optimal interpolation kernel, rather than just a prefilter. We turn our attention to this problem now, explicitly considering sensor noise and rational interpolation factors as well. Note that bold faced indices herein indicate two-vectors – i.e.,  $\mathbf{n} = (n_1, n_2) \in \mathbb{Z} \times \mathbb{Z}$ .

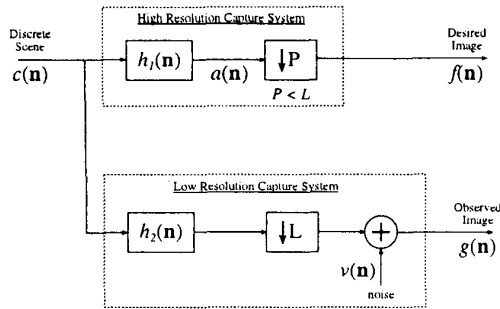


Figure 2: Discrete approximation of the image capture system.

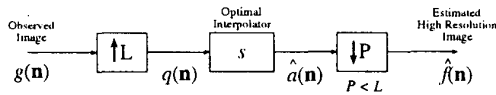


Figure 3: Interpolation with  $s$  to provide optimal estimate,  $\hat{f}(\mathbf{n})$ , of the desired, high resolution image.

To incorporate sensor knowledge into the interpolation problem, we must assume a model of the image capture system(s). As described in [7], many of the effects in a real-world, image capture system are nonlinear and/or shift-varying. Despite this fact, we have found the simple, discrete model shown in Fig. 2 to be concise and effective in our research. The terms  $h_1(\mathbf{n})$  and  $h_2(\mathbf{n})$  represent FIR blurs, where the high resolution blur,  $h_1(\mathbf{n})$ , is more spatially localized than the low resolution blur,  $h_2(\mathbf{n})$ . The term  $v(\mathbf{n})$  represents additive noise from the low resolution sensor. Note that  $P$  and  $L$ , where  $P < L$ , are assumed to be relatively prime.

The problem now is to find an interpolator  $s$ , as shown Fig. 3, that provides an optimal estimate,  $\hat{f}(\mathbf{n})$ , of the desired, high resolution image  $f(\mathbf{n})$ . Note that  $\hat{a}(\mathbf{n})$  in Fig. 3 refers to  $a(\mathbf{n})$  of Fig. 2. Given Figs. 2 and 3, we seek  $s$  to minimize

$$\mathcal{E}_f(\mathbf{n}) = E \left\{ (f(\mathbf{n}) - \hat{f}(\mathbf{n}))^2 \right\} \quad (3)$$

for all  $\mathbf{n}$ . We assume that  $c(\mathbf{n})$  is wide sense stationary (WSS) with covariance  $r_{cc}(\mathbf{k})$  and that the noise,  $v(\mathbf{n})$ , is uncorrelated with  $c(\mathbf{n})$ . Under the assumption that  $c(\mathbf{n})$  is WSS, both  $g(\mathbf{n})$  and  $f(\mathbf{n})$  are also WSS since decimation preserves WSS. (It is well known that WSS is not necessarily an accurate assumption for image processing. Such limitations, however, can be addressed with adaptive interpola-

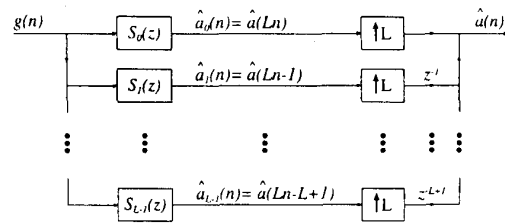


Figure 4: Bank of optimal interpolation filters.

tion algorithms [8].)

In tackling this problem, there are two issues that we consider. First, note that finding  $s$  to minimize

$$\mathcal{E}_a(\mathbf{n}) = E \left\{ (a(\mathbf{n}) - \hat{a}(\mathbf{n}))^2 \right\} \quad (4)$$

for all  $\mathbf{n}$  effectively minimizes  $\mathcal{E}_f(\mathbf{n})$  of (3) for all  $\mathbf{n}$  as well. This is evident since the MMSE of  $\mathbf{y}$  is unique. This fact will make our derivations simpler since we can neglect the factor of  $P$  decimator in Fig. 3. In other words, the optimal interpolator for factor of  $L$  interpolation is also optimal for  $L/P$  interpolation. The second issue is that the input to the interpolator –  $q(\mathbf{n})$  into  $s$  in Fig. 3 – is *not* stationary because of the factor of  $L$  upsampler. We address this issue in the next section.

### 3. SOLUTION

As the input to the interpolator  $s$  is not stationary, the standard Wiener filter solution is not immediately applicable. We can proceed in two ways that are in fact equivalent. For brevity, we describe only our intuitive approach here. Another, more rigorous approach can be carried out using properties of random processes in multirate systems [9], i.e., cyclic Wiener filtering [10]. Using a few multirate identities, it can be shown that the two approaches yield equivalent results [8]. To prevent excessive notation, we will limit our presentation in this section to signals over a single index – i.e., rather than  $g(\mathbf{n})$  with  $\mathbf{n} = (n_1, n_2)$ , we will consider just  $g(n)$ . The extension to images (signals over two indices) is straightforward.

Referring again to Figs. 2 and 3, we seek  $s$  to estimate  $a(n)$  given  $g(n)$ . The signal  $a(n)$  is sampled at  $L$  times the rate of  $g(n)$ , so for every sample of  $g(n)$  we must estimate  $L$  samples of  $a(n)$ . Although  $q(n)$ , the  $L$ -upsampled version of  $g(n)$ , is not stationary, both  $g(n)$  and  $a(n)$  are. This leads us to propose an optimal interpolator composed of a bank of  $L$  (FIR)



Figure 5: Equivalent forms for a section of the  $i^{\text{th}}$  branch in Fig. 4.

filters, where each such filter,  $s_i$ , produces the estimate  $\hat{a}_i(n) = \hat{a}(Ln - i)$  for  $i = 0, 1, \dots, L - 1$ . The  $L$  polyphase processes denoted by  $\hat{a}(Ln - i)$  must then be appropriately interleaved to produce the complete estimate  $\hat{a}(n)$ . This process is illustrated in Fig. 4, where the filters  $s_i(n)$  are represented by their  $z$ -transforms,  $S_i(z)$ .

Finding each optimal interpolation kernel  $s_i$  is just a ubiquitous Wiener filtering problem. Letting each  $s_i$  be a  $2N + 1$  point FIR filter (centered on the origin), the optimal coefficients are found by solving the normal equations

$$\sum_{m=-N}^N s_i(m)r_{gg}(k-m) = r_{ag}^i(k), \quad (5)$$

for  $i \in [0, L - 1]$  and  $k \in [-N, N]$ , where

$$r_{gg}(k) = \mathbf{E} \{g(n)g(n+k)\} \quad (6)$$

and where

$$r_{ag}^i(k) = \mathbf{E} \{a(Ln - i)g(n+k)\}. \quad (7)$$

With known sensor and covariance models, (5)-(7) lead to  $L$  linear systems with  $2N + 1$  unknowns each that can be solved to yield the coefficients of  $s_i(n)$  for  $n \in [-N, N]$  and  $i \in [0, L - 1]$ .

Although we have found a bank of  $L$  filters, it is interesting to note, and perhaps evident from Fig. 4, that this bank can be expressed as a single, time invariant filter. Using a common multirate identity, the  $i^{\text{th}}$  branch of Fig. 4 can be represented in the equivalent form of Fig. 5. Applying the identity of Fig. 5 to each branch (and moving the common up-samplers out), it can be seen that Fig. 4 is equivalent to Fig. 6. Finally, we can collapse the branches of Fig. 6 to get Fig. 7, where the single filter is given by

$$S(z) = \sum_{i=0}^{L-1} z^{-i} S_i(z^L). \quad (8)$$

In other words, the optimal filters  $S_i(z)$  for  $i = 0, 1, \dots, L - 1$  are just the  $L$  polyphase components of a single filter  $S(z)$ . Although the polyphase implementation is more computationally efficient, the representation as a single, time invariant filter permits us to display and examine a single impulse response and/or frequency response.

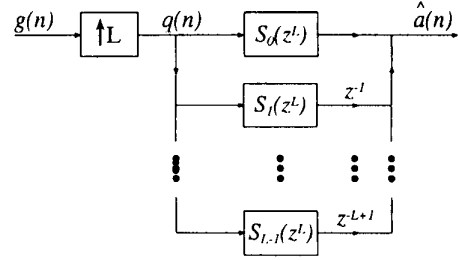


Figure 6: Equivalent representation of the optimal interpolation bank in Fig. 4.

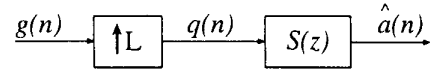


Figure 7: A single, shift-invariant filter for optimal interpolation.

#### 4. RESULTS

We employ the following forms for the sensor blurs from Fig. 2:

$$h_1(\mathbf{n}) = \frac{1}{\mathcal{N}_1} e^{-\tau_1(n_1^2 + n_2^2)} \quad (9a)$$

$$h_2(\mathbf{n}) = \frac{1}{\mathcal{N}_2} e^{-\tau_2(n_1^2 + n_2^2)}, \quad (9b)$$

where  $\mathcal{N}_1$  and  $\mathcal{N}_2$  are normalization factors so that the impulse responses sum to one after truncation. Additionally we assume a nonseparable, exponential covariance model [11] for  $c(\mathbf{n})$  from Fig. 2:

$$r_{cc}(\mathbf{k}) = \rho \sqrt{k_1^2 + k_2^2}. \quad (10)$$

As an example, we consider a factor of  $L = 4$  optimal interpolator using the sensor blurs from (9) with  $\tau_1 = 1.3$  and  $\tau_2 = 0.10$ . The noise variance was chosen to be  $\sigma_v^2 = 0.01$  and  $\rho$  from (10) was 0.95. The size for each of the (polyphase) component interpolators was chosen to be  $13 \times 13$ . The impulse response of the complete  $52 \times 52$  kernel (polyphase components combined) is shown in Fig. 8. The magnitude response of this kernel is shown as a surface in Fig. 9 and as an inverse grayscale image in Fig. 10. The unwrapped phase is shown in Fig. 11. Note that the complete kernel is not linear phase.

Subjective tests were performed using the following rational interpolation factors:

$$L/M \in \{2, 3, 3/2, 4, 4/3, 5, 5/2, 5/3, 5/4, 7, 7/2, 7/3, 7/4\}.$$

$L$	$\tau_1$	$\tau_2$	$\sigma_v^2$	Polyphase Size	Complete Size
2	1	0.25	0.0020	$7 \times 7$	$14 \times 14$
3	1	0.25	0.0035	$9 \times 9$	$27 \times 27$
4	1.3	0.10	0.010	$13 \times 13$	$52 \times 52$
5	1.5	0.10	0.017	$13 \times 13$	$65 \times 65$
7	1.5	0.025	0.034	$17 \times 17$	$119 \times 119$

Table 1: Parameters used to compute optimal interpolation kernels for various upsampling factors used in simulations.  $L$  indicates the upsampling factor,  $\tau_1$  and  $\tau_2$  indicate the parameters of Gaussian sensor blurs from (9), and  $\sigma_v^2$  indicates the variance of the noise term  $v(\mathbf{n})$  from Fig. 2.

The various parameters used to compute the optimal interpolators are summarized in Table 1. Fourteen subjects were shown 42 pairs of images on a computer screen with a black background. Each image pair consisted of one cubic interpolated image and one optimally interpolated image – the type of interpolation was not indicated. The subjects recorded which of each pair they preferred.

After discarding the most and least favorable subjects, 82% (412/504) preferred the optimally interpolated images over the cubic interpolated images. Neglecting the data for facial images, where a softer image is usually preferred, 87% (387/444) of the subjects selected optimal interpolation over cubic interpolation. These results indicate that significant subjective performance improvements can be obtained by interpolating with the sensor optimal kernels. Note that we do not include any example images in this paper as the reproduction process tends to degrade image quality. It is also worth noting that the optimal interpolators, when implemented in polyphase form, require less computation than unoptimized cubic interpolation, such as MATLAB's `interp2(..., '*cubic')` function.

## 5. CONCLUSIONS

In this paper, we construct MMSE interpolators based upon a model of the image capture system. The optimal interpolation kernels are quite long compared to traditional kernels and exhibit nonlinear phase. Experiments indicate that optimal interpolation outperforms cubic interpolation in terms of subjective image quality, without a significant increase in computational cost.

## 6. REFERENCES

- [1] J. R. Price and M. H. Hayes III, "Optimal pre-filtering for improved image interpolation," in *Proc. 32nd Asilomar Conf. on Signals, Systems, and Computers*, vol. 2, pp. 959–963, 1998.
- [2] J. P. Oakley and M. J. Cunningham, "A formula for least-squares projection and its applications in image reconstruction," in *ICASSP*, vol. 3, pp. 1602–1605, 1989.
- [3] J. Allebach and P. W. Wong, "Edge-directed interpolation," in *ICIP*, vol. 3, pp. 707–710, 1996.
- [4] L. Wood and R. A. Schowengerdt, "Restoration for sampled image systems," in *Applications of Digital Signal Processing IX*, vol. SPIE-697, pp. 333–340, 1986.
- [5] S. Carrato, G. Ramponi, and S. Marsi, "A simple edge-sensitive image interpolation filter," in *ICIP*, vol. 3, pp. 711–714, 1996.
- [6] P. W. Wong and C. Herley, "Area-based interpolation for scaling of images from a CCD," in *ICIP*, vol. 1, pp. 905–908, 1997.
- [7] R. Short, D. Williams, and A. E. Jones, "Image capture simulation using an accurate and realistic lens model," in *Electronic Imaging*, vol. SPIE-3650, 1999.
- [8] J. R. Price, *A Framework for Adaptive Image Interpolation*. PhD thesis, Georgia Institute of Technology, 1999.
- [9] V. P. Sathe and P. Vaidyanathan, "Effects of multirate systems on the statistical properties of random signals," *IEEE Trans. on Signal Processing*, vol. 41, no. 1, pp. 131–146, 1993.
- [10] W. A. Gardner, "Cyclic wiener filtering: Theory and method," *IEEE Trans. on Communications*, vol. 41, no. 1, pp. 151–163, 1993.
- [11] A. K. Jain, *Fundamentals of Digital Image Processing*. Prentice-Hall, Inc., 1989.

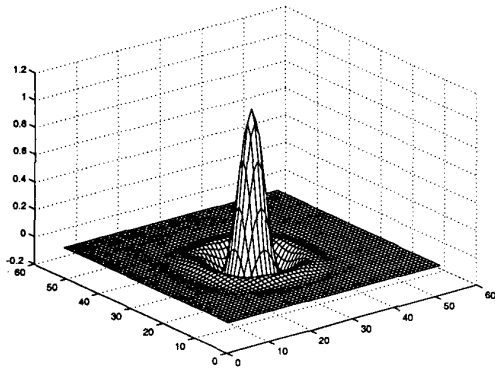


Figure 8: Impulse response of optimal interpolator (polyphase components combined) for factor of four interpolation.

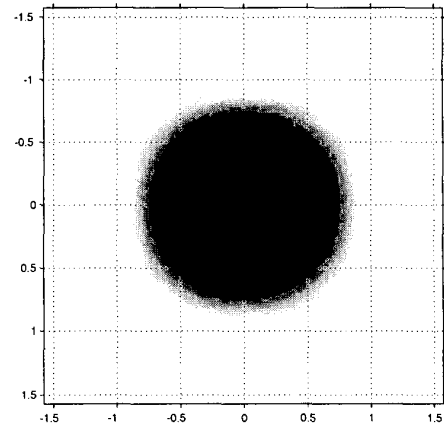


Figure 10: Normalized frequency response magnitude, shown as image, for factor of four interpolator from Fig. 8. Black indicates 1.0, white indicates 0.0.

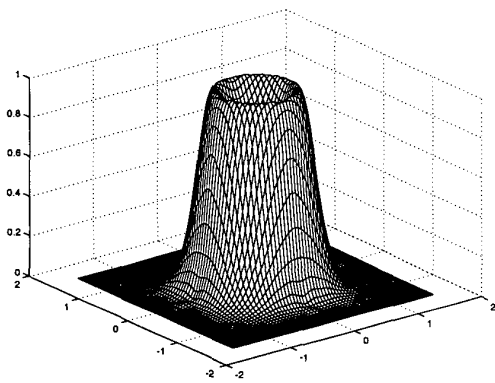


Figure 9: Normalized frequency response magnitude for factor of four interpolator from Fig. 8.

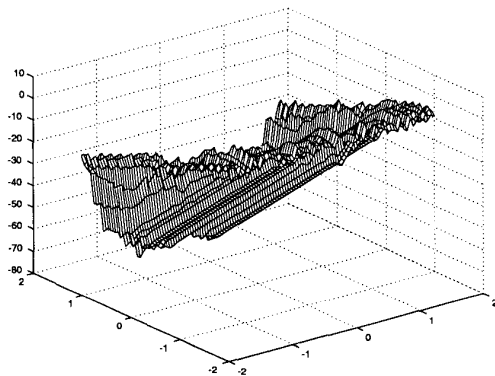


Figure 11: Phase of frequency response for the factor of four interpolator from Fig. 8.